The unique OMI HCHO/NO$_2$ feature during the 2008 Beijing Summer Olympics: implications for ozone production sensitivity

J. C. Witte[a,b**], B. N. Duncan[b], A. R. Douglass[b], T. P. Kurosu[c], K. Chance[c], and C. Retscher[d]

[a] Science Systems and Applications Incorporated, 10210 Greenbelt Road, Suite 600, Lanham, MD 20706, USA, ph:301-614-5991, fx:301-614-5903, email:Jacquelyn.witte@nasa.gov
[b] Atmospheric Chemistry and Dynamics Branch, NASA Goddard Space Flight Center, Greenbelt, MD 20771, USA
[c] Harvard-Smithsonian Center for Astrophysics, 60 Garden Street, Cambridge, MA 02138, USA
[d] Goddard Earth Sciences and Technology Center, University of Maryland Baltimore County, 5523 Research Park Drive, Suite 320, Baltimore, MD 21228, USA

[**] *Corresponding author submitted to Atmospheric Environment*

Abstract

In preparation of the Beijing Summer Olympic and Paralympics Games, strict controls were imposed between July and September 2008 on motor vehicle traffic and industrial emissions to improve air quality for the competitors. We assessed chemical sensitivity of ozone production to these controls using Ozone Monitoring Instrument (OMI) column measurements of formaldehyde (HCHO) and nitrogen dioxide (NO$_2$), where their ratio serves as a proxy for the sensitivity. During the emission controls, HCHO/NO$_2$ increased and indicated a NO$_x$-limited regime, in contrast to the same period in the preceding three years when the ratio indicates volatile organic carbon (VOC)-limited and mixed NO$_x$-VOC-limited regimes. After the emission controls were lifted, observed NO$_2$ and HCHO/NO$_2$ returned to their previous values. The 2005-2008 OMI record shows that this transition in regimes was unique as ozone production in Beijing was rarely NO$_x$-limited. OMI measured summertime increases in HCHO of around 13% in 2008 compared to prior years, the same time period during which MODIS vegetation indices increased. The OMI HCHO increase may be due to higher biogenic emissions of HCHO precursors, associated with Beijing's greening initiative for the Olympics. However, NO$_2$ and HCHO were also found to be well-correlated during the summer months. This indicates an anthropogenic VOC contribution from vehicle emissions to OMI HCHO and is a plausible explanation for the relative HCHO minimum observed in August 2008, concurrent with a minimum in traffic emissions. We calculated positive trends in 2005-2008 OMI HCHO and NO$_2$ of about $+1 \times 10^{14}$ molec cm^{-2} and $+3 \times 10^{13}$ molec cm^{-2} per month, respectively. The positive trend in NO$_2$ may be an indicator of increasing vehicular traffic since 2005, while the positive trend in HCHO may be due to a combined increase in anthropogenic and biogenic emissions since 2005.

Keywords: Air Quality, OMI, NO$_2$, HCHO, Beijing Olympics, Ozone abatement

1. Introduction

In 2001, Beijing, China won the bid to host the 2008 Olympics (August 8-22, 2008) and Paralympics (September 6-17, 2008) (hereafter referred to as the 'Games'), prompting health

47 concerns because of the city's poor air quality, which has worsened in the past several decades
48 from rapid industrialization, population growth, and urbanization (Akimoto, 2003; Molina and
49 Molina, 2004; Hao and Wang, 2005). Aware of Beijing's air quality issues, the Chinese
50 government implemented aggressive short-term strategies to improve air quality during the
51 Games between July and September 2008.
52   Nitrogen oxides (NO_x = $NO+NO_2$), volatile organic compounds (VOCs), and ozone (O_3) are
53 among the important players in gas-phase air pollution affecting Beijing. In the presence of
54 sunlight, NO_x and VOCs are the main ingredients for the formation of high levels of surface
55 ozone (Haagen-Smit, 1952; Seinfeld, 1989), which has detrimental effects on human health
56 (Hallet, 1965; Young et al., 1964; Stokinger, 1965). Photochemical oxidation of VOCs, primarily
57 initiated by the hydroxyl radical (OH), produces organic peroxy radicals (RO_2), adding to the
58 catalytic cycling of NO to NO_2 and the formation of ground-level ozone (Zhang et al., 2004).
59 Oxidation of NO_2 to nitric acid and the conversion of RO_2 to peroxides break the set of chain
60 reactions for O_3 production. Ozone production (PO_3) is nonlinearly related to concentrations of
61 its precursors, so that ambient levels of O_3 depend on both the absolute and relative amounts of
62 NO_x and VOC precursors (Duncan and Chameides, 1998 and references therein). Thus,
63 strategies for controlling O_3 are to reduce emissions of either NO_x or VOCs or both (Sillman et
64 al., 1990 and Sillman et al., 1999; Winner et al., 2000). Sillman (1995) used correlations between
65 the afternoon concentrations of various trace gases (e.g., formaldehyde (HCHO) and total
66 reactive nitrogen (NO_y)) to determine the chemical sensitivity of PO_3 to changes in VOCs and
67 NO_x. Martin et al. (2004a) and Duncan et al. (2010) applied the technique of Sillman (1995) to
68 space-based observations, demonstrating that HCHO and NO_2 from the Global Ozone
69 Monitoring Experiment (GOME) and Ozone Monitoring Instrument (OMI) serve as reasonable
70 proxies for *in situ* observations of VOC and NO_y in polluted environments and their ratio is a
71 reasonable indicator of local PO_3 sensitivity.
72   In Beijing, PO_3 primarily is controlled by VOCs (Song et al., 2007; Wang et al. 2008; Xie et
73 al., 2008; Chou et al., 2009), thus efforts to reduce O_3 levels should focus on VOC reduction
74 strategies. Recent *in-situ* studies assessing the impact of emission controls on urban Beijing's air
75 quality found that although ozone precursors decreased during the Games (Wang et al. 2009a;
76 Wang et al., 2009b; Wang et al., 2010a), surface O_3 actually increased (Wang et al. 2010b).
77 Wang et al. (2010b) found that surface O_3 increased 16% during the Games, despite the local
78 pollution controls, citing regional transport of photochemically aged air and less titration of
79 ozone by NO. Reductions in rural O_3 examined by Wang et al. (2009b) imply that the impact of
80 the emission controls was to shift the maximum in PO_3 closer to the urban source. The local O_3
81 increase was an unanticipated consequence of emission reduction strategies and demonstrates the
82 complexity of the interactions among the pollutants that affect Beijing O_3 levels.
83   The Games prompted the ambitious pollution control actions in and around Beijing, providing
84 a unique opportunity to examine their effectiveness in improving ambient air quality. In this
85 study, we use satellite data from OMI for a top-down approach to assess the impact of the
86 controls on PO_3 during the Games. We construct 7-day running means from daily tropospheric
87 NO_2 and total HCHO column data from OMI. We first examine changes in OMI HCHO/NO_2
88 [hereafter referred to as the Formaldehyde to Nitrogen Dioxide Ratio (FNR)] within the Beijing
89 metro region (i.e., $1°\times1°$ grid around the city center) during the period of emission controls (July
90 through September 2008) and compare this FNR with other similar urban cities in China. We
91 then address trends in HCHO and NO_2 as seen by OMI.

92   The satellite data are described in the following section. Section 3 outlines the emission
93   control measures, with a focus on NO_x and VOC controls. Section 4 describes the local
94   meteorology using rawinsondes. Section 5 discusses the effect of the emission controls on the
95   FNR, HCHO and NO_2. We include a discussion on the growing trend we observe in OMI HCHO
96   and NO_2 data due to increases in anthropogenic and biogenic emissions in and around Beijing. A
97   summary follows in section 6.

98
99   **2.   OMI HCHO and NO_2 columns**

100
101   The Ozone Monitoring Instrument (OMI), a nadir-viewing moderate resolution UV/Vis
102   spectrometer is one of the four instruments on NASA's Aura satellite that was launched in July
103   2004 into a sun-synchronous orbit with an equator crossing-time of 13:38 in the ascending node,
104   OMI has a full cross-track swath of 2600 km, containing 60 pixels ranging from 15×30 km^2 at
105   nadir to 42×162 km^2 at the edge of the swath and provides daily global coverage, mapping
106   pollution products on urban scales. All OMI data used in this study have been filtered to remove
107   cloudy scenes, i.e. filtering reflectivities greater than 30%.
108   We use the tropospheric NO_2 columns reported as the vertical column density between the
109   ground and the estimated mean tropopause pressure height of 150 hPa.   The gridding technique
110   of Wenig et al. (2008) weights the NO_2 vertical column densities where multiple pixels overlap
111   and is used to produce gridded data at a horizontal resolution of $0.05° \times 0.05°$, smaller than the
112   pixel size. Data were taken from the Aura Validation Data Center (AVDC) online:
113   http://avdc.gsfc.nasa.gov. Bucsela et al. (2006) report retrieval accuracy estimates for the
114   tropospheric column to be 25%, with a precision error of 0.25×10^{15} molec cm^{-2}.
115   OMI HCHO total column data are binned into $0.25° \times 0.25°$ grids. Chance et al. (2000) showed
116   that HCHO measurements are a very good indicator of VOCs in regions of elevated biogenic
117   activity. Millet et al. (2006) estimated an overall error in the HCHO column data to be 25-31%.
118   Kurosu et al. (2004) provides information on the nonlinear least-squares fitting retrieval
119   algorithm that was originally developed for GOME and SCIAMACHY and adapted for OMI.
120   The HCHO dataset in this study has been de-trended to remove a growing positive trend in the
121   background values over the lifetime of OMI, i.e. a growing dark current effect in the radiance
122   and irradiance spectra.
123   We calculate 7-day running means and monthly averages for HCHO and NO_2 from 2005 to
124   2008. Temporal averaging has been shown to reduce the HCHO measurement uncertainty and
125   noise (Millet et al., 2008). We consider 2005-2007 in order to quantify changes in 2008 relative
126   to previous years. We do not include 2009 results due to the growing dark current that is
127   producing enhanced across-track striping and hot spots over ocean regions in the HCHO
128   measurements and is too big to correct at present.

129
130   **3.   Emission Control Measures affecting HCHO and NO_2**

131
132   We highlight relevant emission control measures (ECM) taken from a detailed summary
133   reported by the United Nations Environment Program (UNEP) (UNEP, 2009).
134   NO_x was among the pollutants targeted for reduction during the Games. Streets et al. (2003)
135   showed that a growing fraction of NO_x emissions in China is due to the rapid growth in vehicle
136   ownership since the latter part of the 1990s. Although there are natural sources of NO_x (e.g.,
137   forest fires, lightning), the combustion of fossil fuels is the major contributor to photochemical

138 pollution in Eastern China (Ohara et al., 2007; Zhang et al., 2007). HCHO also contributes to the
139 formation of photochemical pollution in urban Beijing, as an intermediate product of
140 hydrocarbon photo-oxidation from methane, anthropogenic VOCs, and fossil fuel combustion
141 (Pang et al., 2009; Xie et al. 2008).
142 From July through September 2008, stringent vehicle traffic controls were adopted, such as i)
143 permitting entry into the city for vehicles with odd or even license plates on alternate days, and
144 ii) banning vehicles with high emissions from entering the downtown core (UNEP report, 2009).
145 Additional ECMs that would affect NO_x concentrations include i) reducing power plant
146 emissions by 30% from their levels in June, well beneath the Chinese emission standard, ii)
147 reducing output or shutting down several heavily-polluting factories, and iii) halting all
148 construction activities (UNEP report, 2009).
149 Photo-oxidation of isoprene is another important source of HCHO. Isoprene (C_5H_8), the
150 principal non-methane hydrocarbon (NMHC) emitted from vegetation (Guenther et al., 2006), is
151 one of the most reactive NMHC, with a daytime residency of less than 1 hour against reaction
152 with the OH radical (Trainer et al., 1987). Isoprene can contribute significantly to the total VOC
153 reactivity in urban environments (Chameides et al., 1992). It has been shown that OMI HCHO
154 can be used as a surrogate measure of isoprene's role in ozone formation, particularly in areas of
155 high biogenic activity (Chance et al., 2000; Millet et al, 2008).
156 As part of Beijing's bid for the 2008 Games, an ambitious tree-planting program was initiated
157 in 2001, with the goal of increasing the green coverage in the Beijing urban area by up to 40%
158 (UNEP report, 2009). Between 2001 and 2007, UNEP reported that approximately 8,800
159 hectares of green space were developed using more than 30 million trees and bushes.
160 Consequently, the vegetation cover in Beijing increased significantly over the past decade. The
161 proportion of green space in 2006 increased by 42.5% of the total urban area compared to 2001
162 (Beijing Bureau of Statistics, 2007). The main species of green cover in Beijing are various
163 broad-leaf deciduous trees, shrubbery, and lawn. Most of them are strong isoprene emitters
164 (Zhang et al., 2000). Pang et al. (2009) and Xie et al. (2008) found that the contribution of *in*
165 *situ* isoprene to local HCHO formation in Beijing is significant during the summer months and
166 can account for 23% - 38% of the local PO_3. Yi et al. (2010) found that photo-oxidation of
167 biogenic NMHCs, i.e,. isoprene and other alkenes, was the major source of HCHO during the
168 Games, with HCHO contributing 22% to the total VOC measurements. Thus, the increasing
169 vegetation coverage is expected to lead to increases of ambient isoprene and its terminal species,
170 HCHO.
171 Several studies have shown that regional emissions significantly impact Beijing's air quality
172 during the summertime when sustained southerly winds are typical (An et al., 2007; Streets et al.,
173 2007; Wang et al., 2008). Thus, some pollution emission controls were also applied on
174 neighboring provinces upwind of Beijing (e.g., Henan, Shanxi, and Hebei provinces located
175 southwest and upwind of Beijing) and in the neighboring city of Tianjin, where traffic
176 restrictions similar to Beijing's were instituted.
177
178 **4. Local Weather Conditions**
179
180 Regional meteorology, pollution sources and terrain all affect local air pollution in Beijing.
181 The Taihang mountain range to the west and north of Beijing (40°N, 116°E) can trap pollution
182 that would otherwise be exported. To the east of Beijing is the highly urban coastal city, Tianjin,
183 and to the south are the heavily industrialized provinces of Heibei, Shanxi and Shandong. Streets

184 et al. (2007) found that polluted air masses from the south significantly impact Beijing's air
185 quality during the summer months, suggesting that additional emission control measures be
186 applied to provinces south of Beijing in preparation of the Games.
187   We use balloon-borne rawinsonde data launched at 12UT at the Beijing International Airport
188 between 2005 and 2008 from the NOAA/Earth System Research Laboratory (ESRL) data
189 archive. Rawinsondes measure the vertical distribution of temperature, RH, pressure and winds.
190 Figure 1 shows the 7-day running mean of surface temperature, RH, wind speed and wind
191 direction from June to September at 1000 hPa. The lines for each year are color-coded, with
192 2008 shown in black. The months between July and September 2005-2008 exhibit a mean
193 temperature range from $26^\circ C$ at the surface to $17^\circ C$ at 850 hPa, high RH (> 50% from the surface
194 to 850 hPa), relatively low wind speeds (2.2 m/s at the surface to 5.8 m/s at 850 hPa), and
195 surface wind directions typically from the southwest to southeast. The prevailing southerly winds
196 show that Beijing is located directly downwind of the heavily industrialized provinces. The mean
197 profile of wind direction from the surface to 500 hPa is summarized in Table 1 showing winds
198 predominantly from the south from the surface up to 850 hPa and a transition to more northerly
199 winds from 700 hPa to 500 hPa indicating an anti-cyclonic flow that minimizes transport of
200 boundary layer pollution into the free troposphere. Hot and humid weather prevails, creating a
201 favorable environment for O_3 formation (Chameides and Walker, 1973; Sillman et al., 1990).
202   July through September 2008 exhibit typical weather patterns, although UNEP (2009) reported
203 higher than average rainfall in Beijing during the August 2008 Olympics; such higher than
204 average rainfall would be expected to improve air quality. Unfortunately, precipitation data are
205 not available. However, the Beijing Meteorological Bureau showed significant improvement in
206 air quality (e.g., NO_2) even during rain-free days, attributing these reductions to the emission
207 controls in the city (UNEP report, 2009). Wang et al (2010b) measured NO_y and VOCs during
208 the Games and found that while precipitation can explain some of the removal of NO_y, the VOCs
209 were unaffected by wet removal. This lends confidence to our own analysis in which we filter for
210 highly cloudy pixels on the assumption that these may contain precipitation events. Decreases
211 from prior years in the remaining cloud-free data should be represent the impact of emissions
212 reductions. Figure 1 plotted at 925 hPa and 850 hPa (not shown) also show typical summertime
213 values for the 2005-2008 period.
214
215 **5. Analysis**

216   5.1. OMI HCHO/NO_2
217
218   Duncan et al. (2010) was the first study to use the OMI FNR to determine the PO_3 sensitivity
219 in urban environments. Examining the Los Angeles (LA) Basin in summer, they found that
220 FNRs < 1 indicate VOC-limited conditions, while FNRs > 2 indicate NO_x-limited conditions.
221 FNRs between 1 and 2 represent a transition regime (i.e., a mixed VOC-NO_x-limited regime)
222 where both NO_x and VOCs can change ozone production. For this work, we applied these regime
223 definitions to our Beijing region since the VOC speciation determined by Song et al. (2007) and
224 Xie et al. (2008) are similar to that of the LA Basin (Brown et al., 2007). Both cities are major
225 metropolitan regions that experience stagnant meteorological conditions during the summer
226 along with high traffic emissions, resulting in poor air quality.
227   Figure 2 shows 7-day running means of the OMI FNR, and HCHO and NO_2 columns
228 calculated for a $1^\circ \times 1^\circ$ box around the Beijing city center (for reference, Figure 3 shows the

229 spatial extent of our area of interest). During the ECM, the FNRs increased above values
230 typically observed during previous years. In general, during the summer months from 2005 to
231 2007, the FNRs tended towards the VOC -limited and mixed VOC-NO$_x$ -limited regimes
232 (highlighted in grey shading in Figure 2a). During this time period, PO$_3$ may have been sensitive
233 to either VOCs and/or NO$_x$ precursors. An exceptional period is July and August 2008, when
234 FNRs indicated a predominantly NO$_x$-limited regime. This is the only period within the time
235 series where FNR values exceeded 2 for an extended duration. We note that there were only two
236 other episodes (mid-August 2006 and mid-July 2007) where FNR exceeded 2. During the NOx-
237 limited period we would expect reductions in NO$_x$ to lead to reductions in PO$_3$. This is supported
238 by Wang et al. (2010b) who found that PO$_3$ was less sensitive to NO$_x$ during the Olympics,
239 compared to a previous similar study by Chou et al. (2009) which examined the August 2006
240 period. In September 2008, the FNRs indicated a mixed VOC-NO$_x$-limited regime, as compared
241 to the more typical VOC-limited regime seen in earlier years. The peak is attributed to a
242 combination of a minimum in NO$_2$ due to pollution controls (Figure 2c) and a relative peak in
243 HCHO (Figure 2b).
244   Beijing is typically in a VOC-limited regime with low HCHO and high NO$_2$ column amounts
245 from mid-autumn to summer (October through June) for all years. Under these conditions, PO$_3$ is
246 expected to be sensitive to VOCs and respond less to changes in NO$_x$. This is consistent with
247 model results reported by Fu et al. (2007). These results for northern China show increases in
248 surface O$_3$ during this time period, with PO$_3$ being sensitive primarily to VOCs.
249   We repeated the analyses over a smaller 0.5°×0.5° grid over Beijing's downtown core and the
250 overall conclusions remain unchanged, indicating reasonable spatial homogeneity within our
251 sampling domain. The major advantage of choosing the larger 1°×1° grid size is that there are
252 fewer data gaps.
253
254   5.2. Unique NO$_x$-Limited Case
255
256   From Figure 2a we observe a peak period between 2008/06/29 and 2008/08/15 where the FNR
257 often exceeds 2 - well within the time period of enforced emission measures. Table 2
258 summarizes various statistics using data in Figure 2 during this time period of enhanced FNRs.
259 2008 stands out as having the highest HCHO and FNRs, as well as the lowest NO$_2$. In the case of
260 NO$_2$, the 3.73×10^{15} molec cm^{-2} minimum in 2008 is the lowest recorded mean column amount
261 during our study period. Table 2 shows the standard deviation and skewness of NO$_2$ during the
262 peak period are also a relative minimum indicating reduced variability, relatively fewer high
263 values, and therefore greater clustering about the mean.
264   We plot the spatial variability of the FNR within a 1°×1° domain around Beijing averaged over
265 the peak period in Figure 3. We observe that within Beijing's provincial boundaries the peak
266 period between 2005 and 2007 reveal a dominant VOC-limited regime, with FNRs < < 1 (darker
267 blue contours) intensified around and slightly south of the city center (marked by the asterisk).
268 This FNR gradually shifted to a mixed VOC-NO$_x$-limited regime (green) away from the city
269 center. Here biogenic VOC sources dominate and the O$_3$ production is sensitive to NO$_x$ in the
270 photochemically aged urban plume (Duncan and Chameides, 1998). This is consistent with
271 previous measurement studies showing that ozone production in the Beijing urban area is VOC-
272 limited (Chou et al., 2009), while the ozone production in surrounding suburban and rural areas
273 is NO$_x$-limited (Wang et al., 2006).

6

274   During the 2008 peak period, Figure 3 shows that the reductions in NO_2 due to emission
275   controls and concomitant enhancements of FNRS occurred throughout the domain. We observe a
276   strong NO_x-limited regime outside and well within the provincial boundaries (yellow-red). In
277   particular, in 2008 there was a shift in FNR values in the vicinity of the city center (black box)
278   from values less than one, typical of a VOC-limited regime, to FNR between 1 and 2 (light blue
279   to green), indicative of a mixed VOC-NO_x regime.
280   The 7-day running mean of the FNR (Figure 2a) reveals instances during which the FNR
281   exceeded 2, indicating a NO_x-limited regime. We obtain a sense of the uniqueness of these
282   instances by comparing the FNR over Beijing during the Games to FNRs obtained for other
283   polluted urban cities in China. We applied the same set of analyses in Figure 2 to several highly
284   urban regions for comparison: Tianjin-Qinhuangdao, the Shanyang-Yingkou region, the
285   Shijiazhuang to Zhenghou urban/industrial corridor, Shanghai-Nanking, and Hong Kong. We
286   found that maximum summertime OMI FNRs never exceeded 2. Rather, these regions were in
287   mixed VOC-NO_x-limited regimes, similar to the 2005-2007 Beijing summers, and VOC-limited
288   regimes (< 1) during the other seasons. Figure 4 shows the July-August means per year of the
289   FNR over China. Over these megacities (white boxes), including Beijing, we observe VOC-
290   limited regions typical of urban environments (blue). As we move away from megacity centers
291   the first regime shifts to mixed VOC-NO_x-limited (green), and and then to NO_x-limited region
292   indicative of rural (or less industrial) environments (red).

294   5.3. HCHO and NO_2 during the ECM

296   High HCHO (Figure 2b) was typical from June to August for all years. We see that HCHO
297   peaked during the summer months, in association with the seasonal maxima in surface
298   temperatures and biogenic emissions (Fu et al., 2007). Figure 5 shows the high correlation (r^2
299   coefficient $= 0.87$) between OMI HCHO and rawinsonde surface temperatures. The Millet et al.
300   (2008) and Duncan et al. (2010) studies showed that biogenic VOCs play a primary role in the
301   spatial and temporal variability of OMI HCHO in the U.S., however we find evidence that
302   anthropogenic contributions from traffic emissions impact the OMI HCHO measurements over
303   Beijing. We use OMI NO_2 as an indicator of vehicle emissions and note that HCHO also
304   increases with NO_2 during the summer months (Figure 6), suggesting an anthropogenic
305   component to OMI HCHO. When we exclude the July –August 2008 control period, we
306   calculate a positive slope of 0.07 and a reasonable correlation of 0.48. Including the control
307   period reduces the correlation to 0.38 (dotted line), suggesting that the anthropogenic
308   contribution to HCHO has been reduced, relative to biogenic contributions.
309   Figure 7 summarizes the percent changes in monthly HCHO from May to September, relative
310   to 2008. Except for August, all the months in 2008 register increases in HCHO. The last column
311   of Figure 7 shows an average +12% increase in May-September 2008 relative to the past three
312   years (blue) and a +11% increase relative to 2005 (the earliest year, red). Excluding August
313   2008, both these increases jump to 18%. May registers the largest set of increases due to
314   particularly low HCHO in 2006 and 2007. The minimum in August 2008 relative to prior years
315   is interesting. Wang et al. (2010a) observed the lowest NMHC concentrations in August 2008,
316   attributing them to a minimum in vehicle exhaust emissions. Similarly, Yi et al. (2010) measured
317   significant reductions in vehicle emission contributions to ambient HCHO. Although we cannot
318   discriminate the contributions of anthropogenic and biogenic sources of OMI HCHO, the

319 correlation with NO_2 from Figure 6 suggests that reductions in the anthropogenic component of
320 HCHO due to vehicle emissions may explain the August 2008 minimum.
321   From Figure 2c, we find significant reductions in NO_2 during the ECM with a return to
322 average values after the transportation bans were lifted at the end of September. Witte et al
323 (2009) and Mijling (2009) gave a detailed study on OMI NO_2 during the Games. Witte et al.
324 (2009) found an average 43% reduction in the OMI tropospheric column NO_2 between July and
325 September 2008 compared to previous years for the same months due to traffic controls. Using a
326 different analyses approach, Mijling et al. (2009) calculated a 59% reduction of OMI NO_2 in
327 August 2008.
328
329   5.4. HCHO and NO_2 2005-2008 Trends
330
331   We calculate a growing trend in HCHO over Beijing using OMI data since 2005 that is
332 consistent with increases in the biogenic emissions, i.e., Beijing's long-term initiative to expand
333 its green cover, and anthropogenic emissions from increasing vehicular traffic (Streets et al.,
334 2003; Zhang et al., 2007). From Table 2, we observe an increasing mean and minimum, and a
335 reduced skewness from 2005 to 2008 indicating a shift towards higher HCHO during the peak
336 period in FNRs. We calculate an increasing trend in HCHO of $+1 \times 10^{14}$ molec cm^{-2} when we
337 remove the interannual variability by subtracting the monthly mean from the 2005-2008 monthly
338 mean, as shown in Figure 8a. We perform the same analyses on NO_2 (Figure 8b) and, likewise,
339 found a positive trend of $+3 \times 10^{13}$ molec cm^{-2} (not including the emission control period),
340 consistent with an increasing trend in local vehicle and industrial emission sources.
341   We examined the 2003-2008 MODIS-Aqua $1° \times 1°$ monthly mean Normalized Difference
342 Vegetation Index (NDVI) and Enhanced Vegetation Index (EVI) over the Beijing province to see
343 if the increasing trend we observe in HCHO is also apparent in the vegetation indices (VIs). The
344 VIs give a measure of 'greenness' of the Earth's land surface with increasing greenness
345 indicating increased ground coverage by growing vegetation. The VIs complement each other in
346 detecting vegetation changes (Huete et al., 2002). NDVI is chlorophyll sensitive with values
347 ranging from -1 to 1. Values above 0.6 indicate dense green vegetation (Huete et al., 2002). EVI
348 is more responsive to variations in the canopy structure, including leaf area with values greater
349 than 0.4 indicating a high leaf area and greater canopy cover (Huete et al., 2006). These analyses
350 were produced with the Giovanni online data system, developed and maintained by the NASA
351 Goddard Earth Sciences Data Information Services Center (GES DISC) (Acker and Leptoukh,
352 2007). Table 3 summarizes the May to September monthly means using the 2003-2008 VIs. We
353 observe that i) the peak in greenness over the Beijing region occurs in July and August, and ii)
354 2008 is noticeably higher compared to the 2003-2007 mean for each month suggesting enhanced
355 vegetation. The data from Table 3 are plotted in Figure 9, similar to Figure 7. Except for the
356 NDVI in June, all other months show persistent vegetation enhancements in 2008 relative to
357 prior years (blue) and 2005 (red). We find NDVI and EVI increases of 3% and 7%, respectively,
358 between the May-September 2008 mean and the 2003-2007 mean (blue). Concurrent with
359 HCHO, in Figure 7, we also find very high VIs in May 2008, compared to other months and
360 previous years.
361   Interestingly, whereas we observed a decrease in monthly HCHO in August 2008 relative to
362 prior years (Figure 7), the VIs indicate an enhancement in vegetation. This finding is consistent
363 with Wang et al. (2010a) who measured negligible changes in biogenic VOCs during the ECMs

364 in Beijing but calculated significant vehicle-related VOC decreases of 9-40%. This is compelling
365 evidence to suggest that OMI HCHO detected reductions in vehicle-related VOCs.
366   The positive trend in OMI HCHO and the enhancements in the VIs in 2008 relative to prior
367 years are not seen in other regions. We performed the same set of analyses shown in Figures 7
368 and 8 for Hong Kong, the Southeast US, Shanghai, and Seoul. These regions do not reveal a
369 clear positive trend or persistent VI enhancements, compared to Beijing.
370   If this increasing trend in HCHO continues it will undoubtedly affect Beijing's PO_3 sensitivity.
371 Aside from the temporary reductions gained by controlling direct emissions, further reductions
372 from natural sources will be a challenge. The pre-Games study by Chou et al. (2009) found that
373 biogenic VOCs, mostly in the form of isoprene, accounted for 22% of the PO_3 sensitivity to all
374 measured VOC species in August 2006, recommending that Beijing's ambitious tree planting
375 program consider tree species with lower isoprene emission rates as an additional means of
376 controlling ozone formation. The most recent evaluation by Wang et al (2010a) found that while
377 the ambient concentrations and PO_3 sensitivity to anthropogenic VOCs were both reduced during
378 the ECM, conversely the contributions of biogenic sources to HCHO and PO_3 sensitivity to
379 isoprene increased.
380

381 **6. Summary**
382

383   The Games in Beijing offered a real-world experiment of the effectiveness of VOC and NO_x
384 emission reductions on the chemical sensitivity of ozone formation as detected from space.
385 Duncan et al. (2010) showed that the ratio of OMI HCHO and NO_2 (i.e., the "FNR") serves as a
386 credible proxy for the ratio of VOCs and NO_x, an indicator of the sensitivity of ozone formation.
387 Following Duncan et al., we used the long-term satellite records of OMI HCHO and NO_2 to
388 show that the FNR increased in Beijing between July and September 2008 mainly as a result of
389 reduced NO_x emissions from vehicles. FNRs greater than 2 were frequently observed, indicating
390 a NO_x-limited regime where ozone formation is sensitive to changes in NO_x and not VOCs.
391 During the same period in the preceding three years, VOC-limited and mixed VOC-NO_x-limited
392 conditions were more typical, in general agreement with limitations estimated from *in situ*
393 observations reported in the literature. This change in regime indicated by OMI data is unique
394 for Beijing. We also detected higher HCHO during most of summer 2008 relative to the past
395 three years, possibly reflecting the ambitious tree planting initiatives to transform Beijing into a
396 greener city in time for the Games. The increasing trend in HCHO since 2005 is consistent with
397 increasing trends in vehicular traffic and biogenic emissions from augmented vegetation cover in
398 and around the city. A decrease in OMI HCHO in August 2008 appears to be consistent with a
399 minimum in traffic emissions. The increasing trend in NO_2 from 2005 to 2008 likely reflects the
400 known increase in vehicular traffic and industrial growth.
401

404

405 **References**

406 Acker and Leptoukh, 2007. J. G. Acker and G. Leptoukh, Online Analysis Enhances Use of
407   NASA Earth Science Data, *Eos Trans.* **88** (2007), pp. 14-17.

408 Akimoto, 2003. H. Akimoto, Global air quality and pollution. *Science* **302** (2003), pp. 1716–
409   1719, doi:10.1126/science.1092666.
410 An et al. 2007. X. An, T. Zhu Z. Wang, C. Li, and Y. Wang, A modeling analysis of a heavy air
411   pollution episode occurred in Beijing, *Atmos. Chem. Phys.* **7** (2007), pp. 3103–3114.
412 Beijing Bureau of Statistics, 2007. Beijing Bureau of Statistics, Beijing Statistics Yearbook
413   2007, China Statistics Press, Beijing (2007) (in Chinese).
414 Bucsela et al., 2006. E. Bucsela, E. Celarier, M. Wenig, J. Gleason, P. Veefkind, K.F. Boersma,
415   and E. Brinksma, Algorithm for NO_2 vertical column retrieval from the Ozone Monitoring
416   Instrument, *IEEE Transactions on Geoscience and Remote Sensing* **44** (2006), pp. 1245-
417   1258.
418 Biesenthal et al., 1997. T. Biesenthal, Q. Wu, P. Shepson, H. Wiebe, K. Anlauf, and G. Mackay,
419   A study of relationships between isoprene, its oxidation products, and ozone, in the lower
420   Fraser Valley, BC, *Atmospheric Environment* **31** (1997), pp. 2049 – 2058.
421 Brown et al., 2007. S. G. Brown, A. Frankel, and H. R. Hafner, Source apportionment of VOCs
422   in the Los Angeles area using positive matrix factorization, *Atmospheric Environment* **41**
423   (2007), pp. 227-237.
424 Cavalcante et al., 2006. R.M., Cavalcante, C. S. Campelo, M. J. Barbosa, E. R. Silveira, T. V.
425   Carvalho, and R. F. Nascimento, Determination of carbonyl compounds in air and cancer
426   Risk assessment in an academic institute in Fortaleza, Brazil, *Atmospheric Environment* **40**
427   (2006), pp. 5701-5711.
428 Chameides et al., 1992. W. Chameides et al., Ozone Precursor Relationships in the Ambient
429   Atmosphere, *J. Geophys. Res.* **97** (1992), pp. 6037-6055.
430 Chameides and Walker, 1973. W. Chameides and J. C. G. Walker, A photochemical theory of
431   tropospheric ozone, *J. Geophys. Res.* **78** (1973), pp. 8751-8760.
432 Chance et al., 2000. K. Chance, P. I. Palmer, R. J. D. Spurr, R. V. Martin, T. P. Kurosu, and D. J.
433   Jacob, Satellite observations of formaldehyde over North America from GOME, *Geophys.*
434   *Res. Lett.* **27** (2000), pp. 3461–3464.
435 Chou et al., 2009. C. Chou, C. Tsai, C. Shiu, S. Liu and T. Zhu, Measurement of NOy during the
436   Campaign of Air Quality in Beijing (CAREBeijing-2006): implications for the ozone
437   production efficiency of NOx, *J. of Geophys. Res.* **114** (2009), p. D00G01,
438   doi:10.1029/2008JD010446.
439 Duncan et al., 2010. B. N. Duncan et al., Application of OMI observations to a space-based in
440   indicator of NO_x and VOC controls on surface ozone formation, *Atmospheric Environment*
441   **44** (2010), pp. 2213-2223.
442 Duncan and Chameides, 1998. B. N. Duncan and W. L. Chameides, Effects of urban emission
443   control strategies on the export of ozone and ozone precursors from the urban atmosphere
444   to the troposphere, *J. of Geophys. Res.* **103**(D21), pp. 28159-28179.
445 Fehsenfeld et al., 1992. F. Fehsenfeld et al., Emissions of Volatile Organic Compounds From
446   Vegetation and the Implications For Atmospheric Chemistry, *Global Biogeochemical*
447   *Cycles* **6**(4), pp. 389–430.
448 Feng, Y., et al., 2005. Y. Feng, S. Wen, Y. Chen, X. Wang, H. Lü, X. Bi, G. Sheng, and J. Fu,
449   Ambient levels of carbonyl compounds and their sources in Guangzhou, China.
450   *Atmospheric Environment* **39** (2005), pp. 1789-1800.
451 Fu et al., 2007. T.-M. Fu, D. J. Jacob, P. I. Palmer, K. Chance, Y. X. Wang, B. Barletta, D. R.
452   Blake, J. C. Stanton, and M. J. Pilling, Space-based formaldehyde measurements as

constraints on volatile organic compound emissions in east and south Asia and implications for ozone, *J. Geophys. Res.* **112** (2007), p. D06312, doi:10.1029/2006JD007853.

Guenther et al. 2006. A. Guenther, T. Karl, P. Harley, C. Wiedinmyer, P. I. Palmer, and C. Geron, Estimates of global terrestrial isoprene emissions using MEGAN (Model of Emissions of Gases and Aerosols from Nature), *Atmospheric Chemistry and Physics* **6** (2006), pp. 3181–3210.

Haagen-Smit, 1952. A. J. Haagen-Smit, Chemistry and Physiology of Los Angeles Smog, *Ind. Eng. Chem.* **44** (6), pp. 1342–1346, doi:10.1021/ie50510a045.

Hallet (1965). W. Hallet, Effect of ozone and cigarette smoke on lung function, *Arch. Environ. Health, 10,* 295-302, 1965.

Hao and Wang, 2005. J. M. Hao and L. T. Wang, Improving urban air quality in China: Beijing case study, *J. Air Waste Manage. Assoc.* **55** (2005), pp. 1298 – 1305.

Huete et al., 2002. A. Huete, K. Didan, T. Miura, E. P. Rodriguez, X. Gao, and L. G. Ferreira, Overview of the radiometric and biophysical performance of the MODIS vegetation indices, *Remote Sensing of Environment,* **83** (1-2) (2002), pp. 195-213.

Huete et al., 2006. A. Huete, K. Didan, Y. E. Shimabukuro, P. Ratana, S. R. Saleska, L. R. Hutyra, W. Yang, R. R. Nemani, and R. Myneni, Amazon rainforests green-up with sunlight in dry season, *Geophys. Res. Lett.,* **33** (2006), p. L06405, doi:10.1029/2005GL025583.

Kurosu et al., 2004. T. P. Kurosu, K. Chance, and C.E. Sioris, Preliminary results for HCHO and BrO from the EOS-Aura Ozone Monitoring Instrument, Passive Optical Remote Sensing of the Atmosphere and Clouds IV, Proc. of SPIE Vol. 5652, doi:10.1117/12.578606.

Martin et al., 2004a. R. V. Martin et al., Evaluation of GOME satellite measurements of tropospheric NO and HCHO using regional data from aircraft campaigns in the southeastern United States, *J. Geophys. Res.* **109** (2004a), p. D24307, doi:10.1029/2004JD004869.

Martin, R. V., A. M. Fiore, and A. Van Donkelaar (2004b), Space-based diagnosis of surface ozone sensitivity to anthropogenic emissions, Geophys. Res. Lett., 31, L06120, doi:10.1029/2004GL019416.

Mijling et al. 2009. B. Mijling, R. J. van der A, K. F. Boersma, M. Van Roozendael, I. De Smedt, I., and H. M. Kelder, Reductions of NO2 detected from space during the 2008 Beijing Olympic Games, *Geophys. Res. Lett.* **36** (2009), p. L13801, doi:10.1029/2009GL038943.

Millet et al. 2008. D. B. Millet, D. J. Jacob, K. F. Boersma, T.-M. Fu, T. P. Kurosu, K. Chance, C. L. Heald, and A. Guenther, Spatial distribution of isoprene emissions from North America derived from formaldehyde column measurements by the OMI satellite sensor, *J. Geophys. Res.* **113** (2008), p. D02307, doi:10.1029/2007JD008950.

Molina and Molina, 2004. M. J. Molina and L. T. Molina, Megacities and atmospheric pollution, *Journal of the Air and Waste Management Association* **5** 4 (2004), pp. 644 – 680.

Ohara et al., 2007. T. Ohara, H. Akimoto, J. Kurokawa, N. Horii, K. Yamaji, X. Yan, and T. Hayasaka, An Asian emission inventory for the period 1980–2020, *Atmos. Chem. Phys.* **7** (2007), pp. 4419-4444.

Pang et al., 2009. X. Pang, Y. Mun, Y. Zhang, X. Lee, and J. Yuan, Contribution of isoprene to formaldehyde and ozone formation based on its oxidation products measurement in

Beijing, China, *Atmospheric Environment* **43** (2009), pp. 2142-2147, doi:10.1016/j.atmosenv.2009.01.022.

Seinfeld, 1989. J. Seinfeld, Urban air pollution: State of the science, *Science* **243** (1989), pp. 745-752.

Sillman, 1999. S. Sillman, The relation between ozone, NOx and hydrocarbons in urban and polluted rural environments, *Atmospheric Environment* **33** (1999), pp. 1821-1845.

Sillman, 1995. S. Sillman, The use of NO_y, H_2O_2, and HNO_3 as indicators for ozone-NO_x-hydrocarbon sensitivity in urban locations, *J. Geophys. Res.* **100 (1995), pp.** 14,175-14,188.

Sillman et al., 1990. S. Sillman, J. Logan, and S. Wofsy, The Sensitivity of Ozone to Nitrogen Oxides and Hydrocarbons in Regional Ozone Episodes, *J. Geophys. Res.* **95** (1990), pp. 1837-1851.

Song et al., 2007. Y. Song, M. Shao, Y. Liu, S. Lu, W. Kuster, P. Goldan, and S. Xie, Source apportionment of ambient volatile organic compounds in Beijing, *Environmental Science and Technology* **41** (2007), pp. 4348–4353.

Stokinger, H., Ozone toxicology: A review of research and industrial experience, *Arch. Environ. Health, 10,* 719-31, 1965.

Streets et al., 2007. D. G. Streets et al., Air Quality during the 2008 Beijing Olympic Games, *Atmospheric Environment* **41** (2007), pp. 480-492.

Trainer et al., 1993. M. Trainer et al., Correlation of ozone with NO_y in photochemically aged air, *J. Geophys. Res.* **98** (1993), pp. 2917–2915.

United Nations Environment Program (UNEP), 2009. Independent Environmental Assessment: Beijing 2008 Olympic Games, *UNEP* (2009), ISBN: 978-92-807-2888-0.

Wang et al., 2010a. B. Wang, M. Shao, S.H. Lu, B. Yuan, Y. Zhao, M. Wang, S.Q. Zhang, and D. Wu, Variation of ambient non-methane hydrocarbons in Beijing city in summer 2008, *Atmos. Chem. Phys.* **10** (2010a), pp. 6087-6096.

Wang et al., 2010b. T. Wang et al., Air quality during the 2008 Beijing Olympics: secondary pollutants and regional impact, *Atmos. Chem. Phys. Discuss.* **10** (2010b), pp. 12433–12463.

Wang et al., 2009a. M. Wang, T. Zhu, J. Zheng, R. Y. Zhang, S. Q. Zhang, X. X. Xie, Y. Q. Han, Y. and Li, Use of a mobile laboratory to evaluate changes in on-road air pollutants during the Beijing 2008 Summer Olympics, *Atmos. Chem. Phys.* **9** (2009a), pp. 8247–8263.

Wang et al., 2009b. Y. Wang, J. Hao, M. B. McElroy, J. W. Munger, H. Ma, D. Chen, and C. P. Nielsen, Ozone air quality during the 2008 Beijing Olympics – effectiveness of emission restrictions, *Atmos. Chem. Phys.* **9** (2009b), pp. 5237-5251.

Wang et al., 2008. Q. Wang, Z. Han, T. Wang and R. Zhang, Impacts of biogenic emissions of VOC and NO_x on tropospheric ozone during summertime in eastern China, *Science of The Total Environment* **395** (2008), pp. 41-49, doi:10.1016/j.scitotenv.2008.01.059.

Wang et al., 2006. T. Wang, A. Ding, J. Gao, and W. S. Wu, Strong ozone production in urban plumes from Beijing, China, *Geophys. Res. Lett.*, **33** (2006), p. L21806, doi:10.1029/2006GL027689.

Wenig et al. 2008. M. O. Wenig, A. M. Cede, E. J. Bucsela, E. A. Celarier, K. F. Boersma, J. P. Veefkind, E. J. Brinksma, J. F. Gleason, and J. R. Herman, Validation of OMI tropospheric NO2 column densities using direct-Sun mode Brewer measurements at NASA Goddard Space Flight Center, *J. Geophys. Res.* **113**, p. D16S45, doi:10.1029/2007JD008988.

542 Winner and Cass, 2000. D. L. Winner and G. R. Cass, Effect of emissions control on the long-
543   term frequency distribution of regional ozone concentrations, *Environ. Sci. Technol.* **34**
544   (2000), pp. 2612–2617.
545 Witte et al., 2009. J. C. Witte, M. R. Schoeberl, A. R. Douglass, J. F. Gleason, N. A. Krotkov, J.
546   C. Gille, K. E. Pickering, and N. Livesey, Satellite observations of changes in air quality
547   during the 2008 Beijing Olympics and Paralympics, *Geophys. Res. Lett.* **36** (2009),
548   doi:10.1029/2009GL039236.
549 Xie et al., 2008. X. Xie, M. Shao, Y. Liu, S. Lu, C. Chang, and Z. Chen, 2008. Estimate of initial
550   isoprene contribution to ozone formation potential in Beijing, China, *Atmospheric*
551   *Environment* **42** (2008), pp. 6000–6010.
552 Young, W., D. Shaw, and D. Bates, Effects of low concentrations of ozone on pulmonary
553   function in man, *J. Appl. Physiol., 19*, 765-8, 1964.
554 Zhang et al., 2007. Q. Zhang et al., NOx emission trends for China, 1995–2004: The view from
555   the ground and the view from space, *J. Geophys. Res.* **112** (2007), p. D22306,
556   doi:10.1029/2007JD008684.
557 Zhang et al., 2000. X. Zhang, Y. Mu, W. Song and Y. Zhuang, Seasonal variations of isoprene
558   emissions from deciduous trees, *Atmospheric Environment* **34** (2000), pp. 3027–3032.
559
560 **Tables and Figures**
561
562 Table 1. Mean wind direction between July and September 2008 at 12Z. The Southern quadrant
563 includes the 90°-270° hemisphere and the Northern quadrant includes 0°-90° and 270°-360°.

Year	Surface (0.06 km)		925 hPa (0.8 km)		850 hPa (~1.5 km)		700 hPa (~ 3 km)		500 hPa (~5.7 km)	
	% South	% North	% South	% North	% South	% North	% South	% North	% South	% North
2008	75.8	14.2	85.7	13.2	61.5	36.3	36.3	54.9	40.2	54.4
2007	75.0	8.7	82.6	17.4	63.0	37.0	30.4	67.4	32.6	58.7
2006	71.7	9.8	72.8	23.9	62.0	34.8	41.3	54.4	41.3	51.1
2005	66.3	13.0	71.7	27.2	60.9	38.0	33.7	65.2	41.3	54.3

564
565
566 Table 2. The mean, standard deviation, skewness, maximum and minimum values of the FNR
567 (HCHO/NO₂), HCHO, and NO₂ calculated during the peak period between June 29 and August
568 15 for 2005 through 2008. Temporal averages are calculated over a 1°×1° box around the Beijing
569 city center.

		2008	2007	2006	2005
HCHO/NO$_2$	Mean	2.32	1.26	1.32	1.10
	Std. Deviation	0.69	0.27	0.34	0.22
	Skewness	1.12	1.15	1.47	1.15
	Max Value	5.09	2.19	2.59	1.71
	Min Value	1.00	0.82	0.78	0.82

		2008	2007	2006	2005
HCHO ($\times 10^{16}$ molec cm^{-2})	Mean	1.46	1.37	1.35	1.33
	Std. Deviation	0.34	0.33	0.34	0.37
	Skewness	-0.03	0.12	0.49	0.73
	Max Value	2.34	2.29	2.37	2.24

	Min Value	0.75	0.68	0.65	0.66
		2008	2007	2006	2005
NO$_2$ ($\times 10^{15}$ molec cm^{-2})	Mean	6.44	11.00	10.49	12.20
	Std. Deviation	0.88	2.43	2.47	2.62
	Skewness	0.17	0.34	0.72	0.73
	Max Value	7.96	16.30	19.00	18.59
	Min Value	3.73	7.75	6.68	8.81

570
571 Table 3. 2003-2008 MODIS-Aqua V005 NDVI and EVI monthly values (unitless) from May to
572 September for 2005, the mean from 2003-2007, and 2008. The area average encompasses the
573 Beijing provincial borders from 39.5N-40.5N and 115.5E-117.5E.
574

	May		June		July		August		Sept.	
	NDVI	EVI	NDVI	EVI	NDVI	EVI	NDVI	EVI	NDVI	EVI
2005	0.454	0.272	0.563	0.334	0.678	0.430	0.713	0.439	0.618	0.317
Avg. (2003-2007)	0.459	0.274	0.554	0.337	0.692	0.437	0.717	0.442	0.640	0.352
2008	0.474	0.290	0.546	0.345	0.711	0.450	0.726	0.451	0.651	0.370

575
576
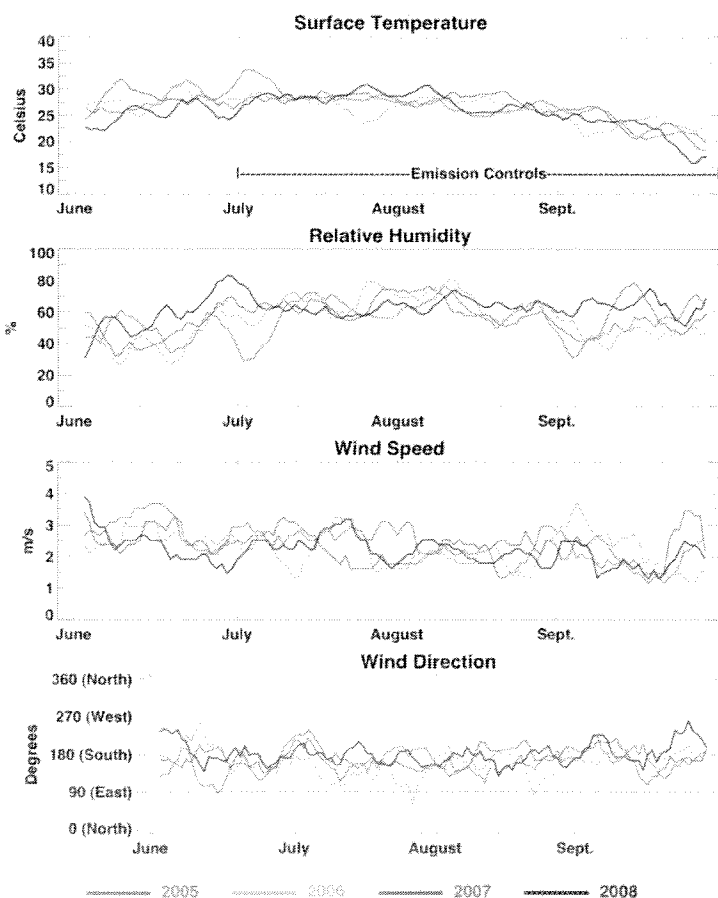
577

578

579   Figure. 1 7-day running mean of surface temperature [Celsius], relative humidity [%], wind

580   speed [m/s], and wind direction [degrees] for 2005 (blue), 2006 (green), 2007 (red), and 2008

581   (black) at 1000 hPa. Data are taken from balloon-borne rawinsondes launched daily at 12Z at the

582   Beijing International Airport (39.93°N, 116.28°E). The x-axis divides the data into its respective

583   months.

584

584
585 a
586
587
588
589
590
591
592
593
594
595
596
597
598
599 b
600
601
602
603
604
605
606
607
608
609
610 c
611
612
613
614
615
616
617
618
619
620
621
622
623
624
625
626
627
628
629
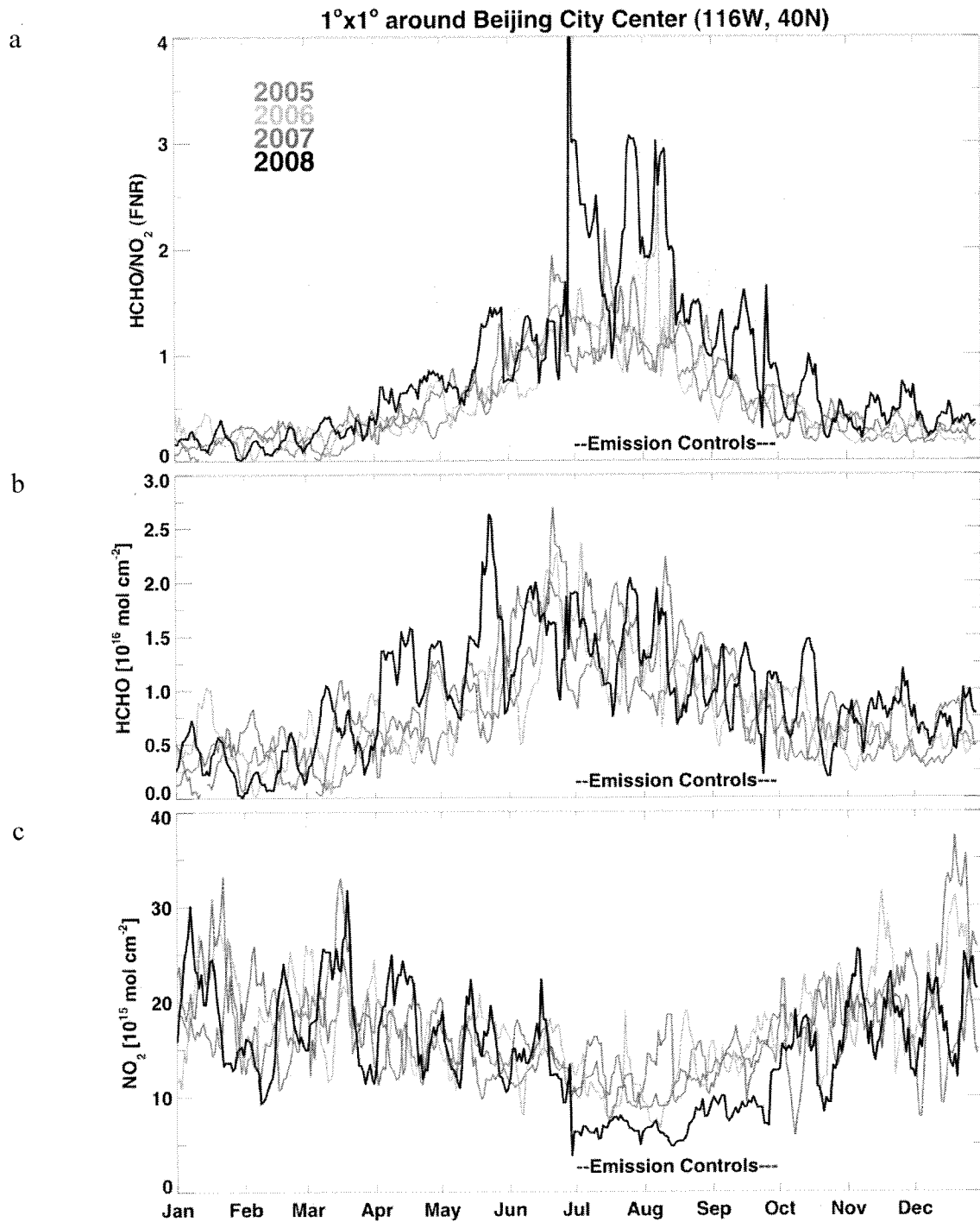
Figure 2. 7-day running means of (a) FNR, (b) HCHO total columns [10^{16} molec cm^{-2}], and (c) tropospheric NO$_2$ columns [10^{15} molec cm^{-2}]. The spatial average is a $1°×1°$ area around the Beijing city center (39.9°N, 116.92°E) and color coded by year similar to Figure 1. The grey shading in (a) identifies the VOC-NO$_x$-limited regime (FNRs between 1 and 2). The time period of the strict emission controls between July and September 2008 is marked on each plot.

629
630

June 29 - August 15 HCHO/NO$_2$ Mean
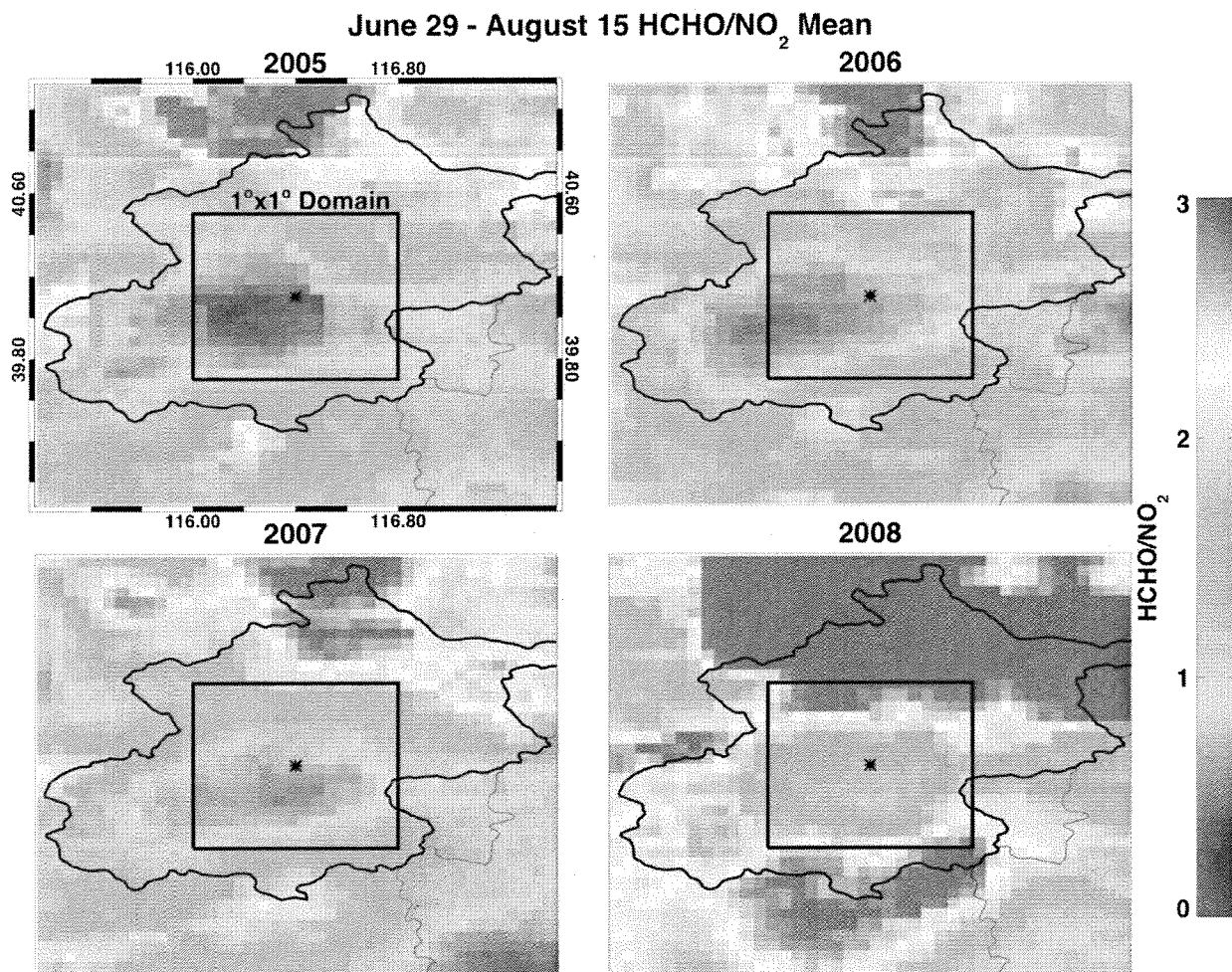
631
632
633   Figure 3. The FNR averaged over the June 29 to August 15 peak period for 2005 (upper left),
634   2006 (upper right), 2007 (lower left), and 2008 (lower right) over the Beijing province. The
635   black box is our 1°×1° domain around the Beijing city center, marked by an asterisk (116°E,
636   40°N). The thick black outline highlights the provincial boundary of Beijing.
637
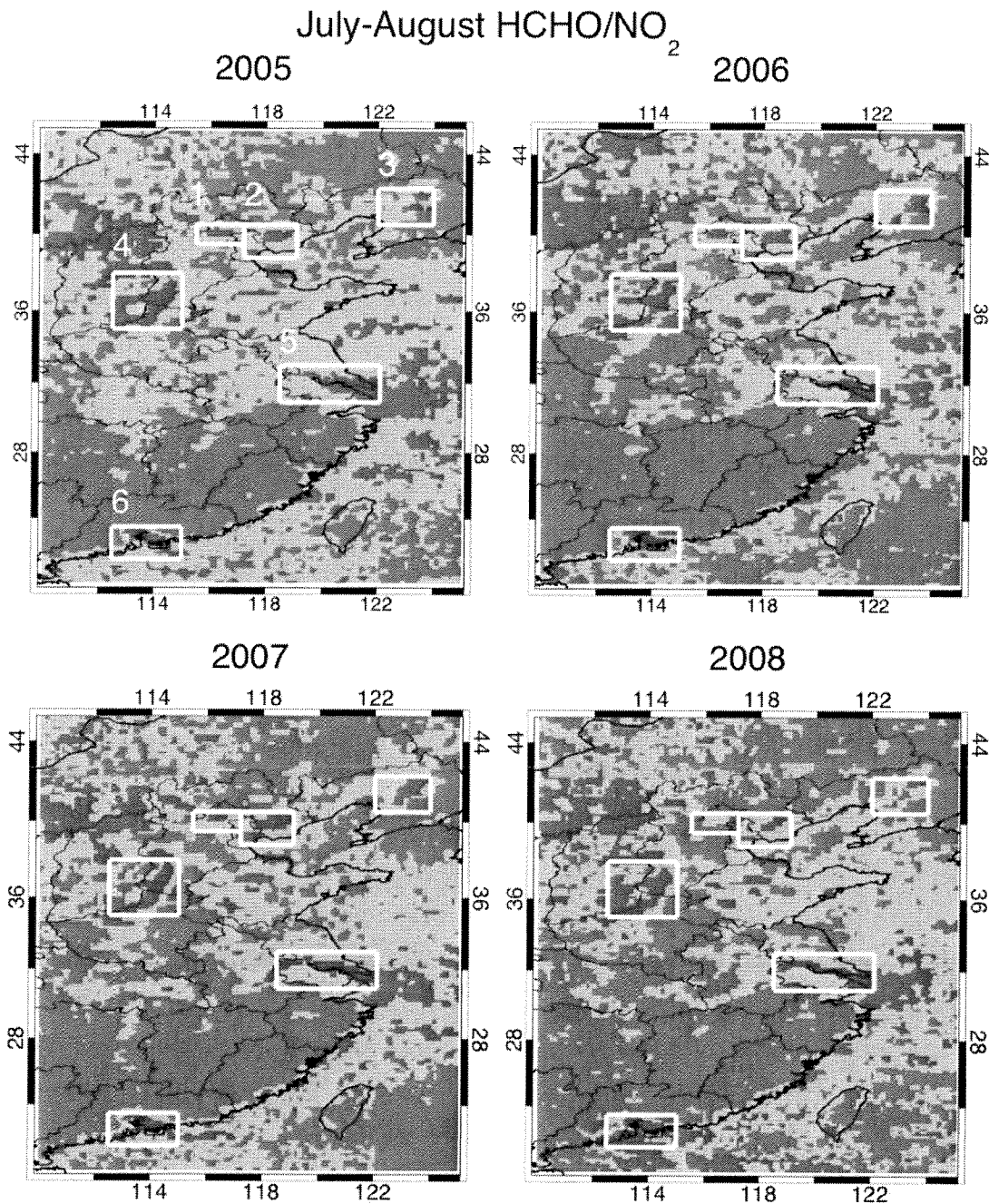
Figure 4. July-August mean of the FNRs for 2005 through 2008. The blue areas show FNRs less than 1, green indicate FNRs between 1 and 2, and red for FNRs greater than 2. Numbers in the top left panel indicate the white-boxed regions of interest: 1= Beijing province [115°N-117°N, 115°E-117°E], 2 = Tianjin-Qinhuangdao [38.5°N-41.0°N, 116.5°E-119.5°E], 3= Shanyang-Yingkou region [40.5°N-42.5°N, 122°E-125°E], 4 = Shijiazhuang to Zhenghou industrial corridor [35.0°N-38.0°N, 112.5°N-115.0°E], 5 = Shanghai-Nanking region [30.2°N-32.7°N, 118.5°E-112.5°E], and 6 = Hong Kong [21.5°N-23.5°N, 112.5°E-115°E].

18

646
647
648
649
650
651
652
653
654
655
656
657
658
659
660
661   Figure 5. Monthly HCHO vs. surface temperature from the rawinsondes. The filled squares
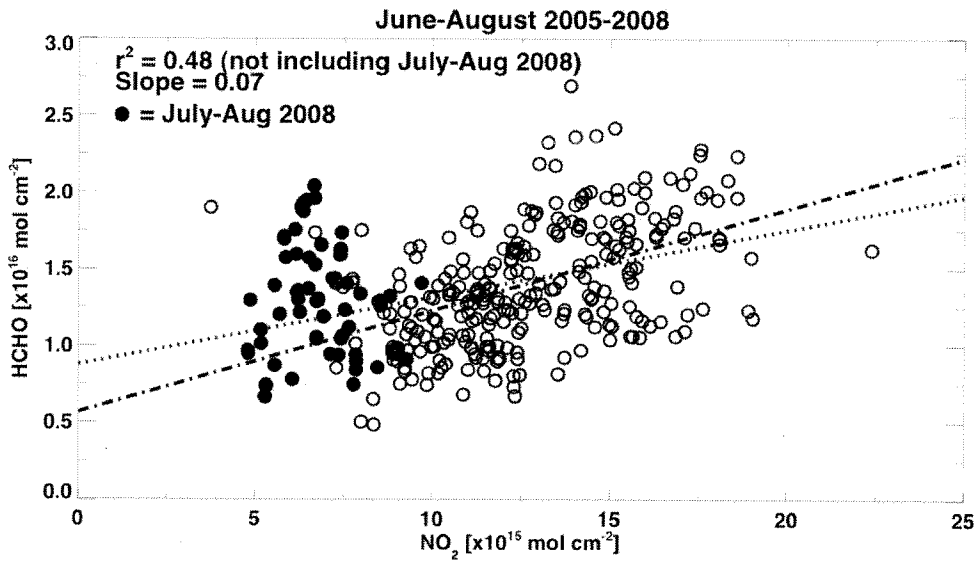662   indicate the June, July, and August 2008 monthly data.
663
664
665
666
667
668
669
670
671
672
673
674
675
676
677
678
679
680
681
682   Figure 6. HCHO vs. NO$_2$ for June-August 2005-2008. 7-day running means are plotted over a
683   1°×1° area around urban Beijing. Dash-dot line is the linear fit to the data, excluding the July-
684   August 2008 control period. The dotted line includes the control period with an r^2 value of 0.38.

685
686
687
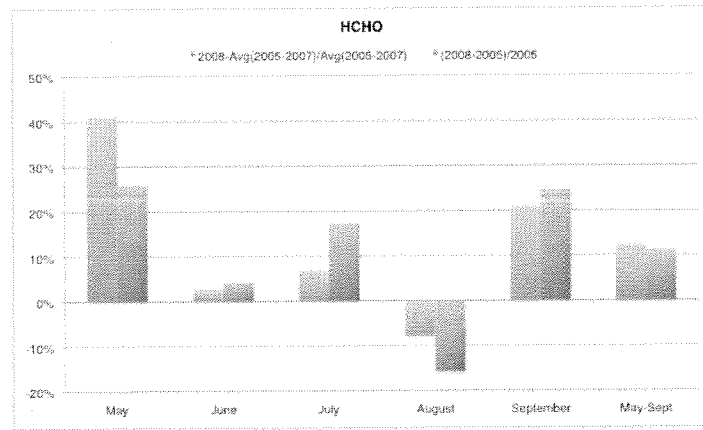688
689
690
691
692
693
694
695
696
697
698

699 Figure 7. Monthly mean differences of HCHO from May to September, recorded as percent
700 differences relative to 2008. The last row is the average percentage change between May and
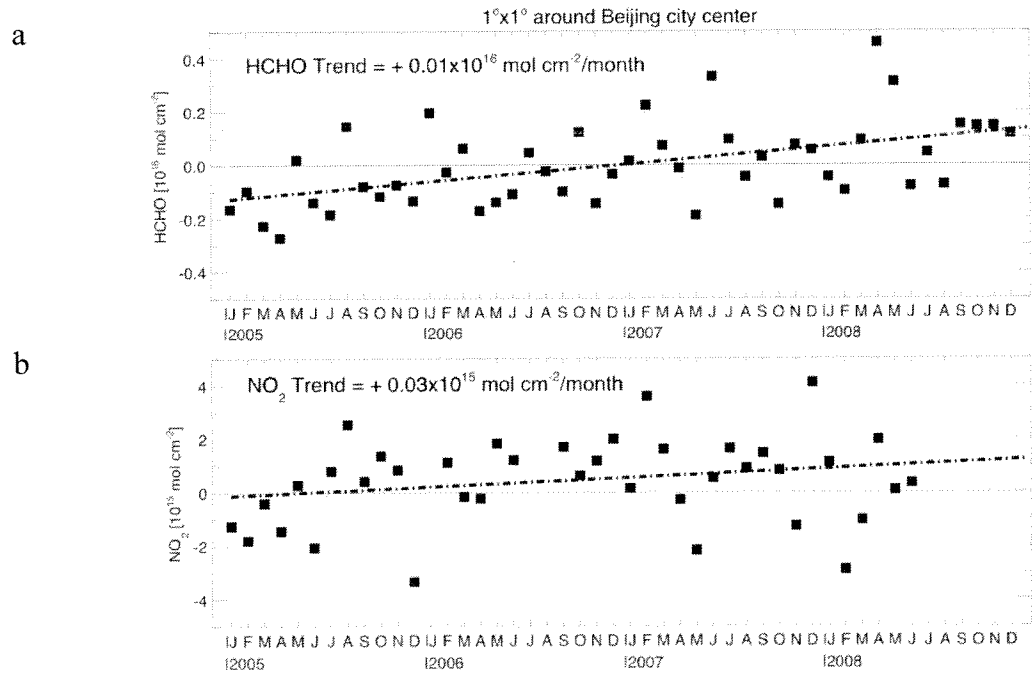701 September 2008 relative to 2005.
702
703
704
705 a
706
707
708
709
710
711
712
713

714 b
715
716
717
718
719
720
721
722
723
724
725
726 Figure 8. Monthly HCHO (a) and NO_2 (b) minus the monthly mean between 2005-2008 over a
727 $1° \times 1°$ area around the Beijing city center. Linear fits to the data (dashed lines) indicate small
728 increasing trends. The NO_2 trend excludes the Olympic time period.
729
730

20

730
731
732
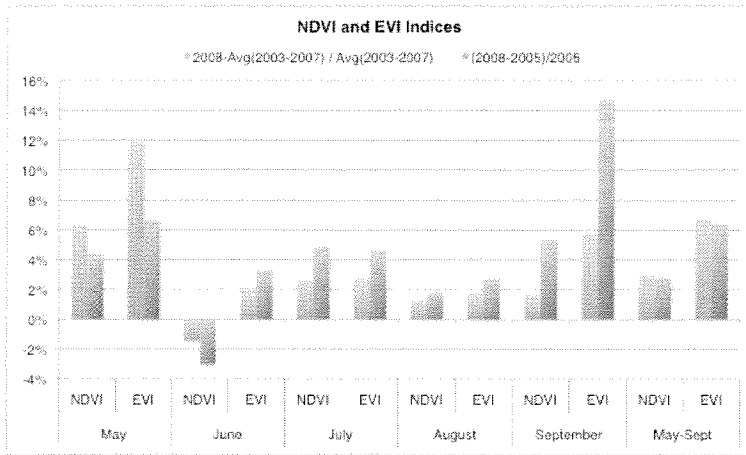
733
734
735 Figure 9. 2003-2008 MODIS-Aqua V005 NDVI and EVI monthly mean percentage differences
736 relative to 2008, as in Figure 6. The area average encompasses the Beijing provincial borders
737 from 39.5°N-40.5°N and 115.5°E-117.5°E
738
739